Free methionine-(*R*)-sulfoxide reductase from *Escherichia coli* reveals a new GAF domain function

Zhidong Lin*, Lynnette C. Johnson*, Herbert Weissbach[†‡], Nathan Brot[§], Mark O. Lively*, and W. Todd Lowther*

*Center for Structural Biology, Department of Biochemistry, Wake Forest University School of Medicine, Winston–Salem, NC 27157; [†]Center for Molecular Biology and Biotechnology, Florida Atlantic University, 777 Glades Road, Boca Raton, FL 33431; and [§]Hospital for Special Surgery, Department of Microbiology and Immunology, Weill Medical College of Cornell University, New York, NY 10021

Contributed by Herbert Weissbach, April 24, 2007 (sent for review March 7, 2007)

The reduction of methionine sulfoxide (MetO) is mediated by methionine sulfoxide reductases (Msr). The MsrA and MsrB families can reduce free MetO and MetO within a peptide or protein context. This process is stereospecific with the *S*- and *R*-forms of MetO repaired by MsrA and MsrB, respectively. Cell extracts from an MsrA$^-$B$^-$ knockout of *Escherichia coli* have several remaining Msr activities. This study has identified an enzyme specific for the free form of Met-(*R*)-O, fRMsr, through proteomic analysis. The recombinant enzyme exhibits the same substrate specificity and is as active as MsrA family members. *E. coli* fRMsr is, however, 100- to 1,000-fold more active than non-selenocysteine-containing MsrB enzymes for free Met-(*R*)-O. The crystal structure of *E. coli* fRMsr was previously determined, but no known function was assigned. Thus, the function of this protein has now been determined. The structural similarity of the *E. coli* and yeast proteins suggests that most fRMsrs use three cysteine residues for catalysis and the formation of a disulfide bond to enclose a small active site cavity. This latter feature is most likely a key determinant of substrate specificity. Moreover, *E. coli* fRMsr is the first GAF domain family member to show enzymatic activity. Other GAF domain proteins substitute the Cys residues and others to specifically bind cyclic nucleotides, chromophores, and many other ligands for signal potentiation. Therefore, Met-(*R*)-O may represent a signaling molecule in response to oxidative stress and nutrients via the TOR pathway in some organisms.

methionine oxidation | methionine sulfoxide reductase

Reactive oxygen species cause cellular damage to lipids, DNA and proteins. In proteins this damage includes the oxidation of methionine (Met) to methionine sulfoxide (MetO) (1). The addition of one oxygen atom to either lone pair of electrons of the sulfur atom results in the formation of either the *S*- or *R*-form of MetO. MetO has been implicated in a variety of disease states, and in some instances the reduction or repair of this oxidation to Met restores the biological and enzymatic function of proteins (2). The reduction of MetO is mediated by several families of methionine sulfoxide reductases (Msr). The structures and catalytic mechanisms of the MsrA and MsrB families have been extensively studied (3, 4). Key features of both families are their strict substrate stereospecificity and ability to reduce both free MetO and MetO within a peptide or protein context. The MsrA and MsrB enzymes reduce Met-(*S*)-O and Met-(*R*)-O, respectively. Moreover, these enzymes share a reaction mechanism that involves the formation of a cysteine sulfenic acid intermediate (Cys-SOH) and the subsequent formation and reduction of disulfide bonds which can differ depending on the number of Cys residues present.

The *Escherichia coli* MsrB enzyme creates somewhat of a conundrum. Crude extracts show little MsrB activity, and the recombinant enzyme has significantly lower activity for free Met-(*R*)-O when compared with the MsrA enzymes (5). Thus, it is unclear how MsrB could enable an *E. coli* Met auxotroph to grow on Met-(*R*)-O as a Met source (6). Additional Msr enzymes have been observed which may explain these findings (6–9). Studies with the MsrA$^-$B$^-$ strains of *Escherichia coli* and *Saccharomyces cerevisiae* have most recently revealed or proposed the existence of enzymes specific for free Met-(*R*)-O, free Met-(*S*)-O, peptide Met-(*S*)-O, and a membrane-associated protein(s), which is able to reduce all forms of MetO (7, 8, 10). The Msr with the highest specific activity in the *E. coli* MsrA$^-$B$^-$ soluble extract is the free Met-(*R*)-O reductase (fRMsr). Nothing is currently known about the structure and catalytic mechanism of fRMsr. The specificity of the enzyme for free Met-(*R*)-O may have broad implications for resistance to oxidant stress.

In this study, we have determined the identity of *E. coli* fRMsr through its purification from the MsrA$^-$B$^-$ strain and proteomic analysis. The recombinant enzyme has been expressed, purified, and characterized with regards to its substrate specificity, kinetic parameters, and ability to use the NADPH-thioredoxin (Trx) reductase (TrxR)-Trx reduction system. The fRMsr sequence is highly conserved across bacteria and yeast, but is not found in higher organisms, including humans. The fRMsr domain is part of the large GAF domain family typified by cGMP-binding phosphodiesterases, *Anabaena* adenylyl cyclases, and the *E. coli* transcription factor FhlA (11). These findings suggest that fRMsr represents a GAF domain with enzymatic activity, and that Met-(*R*)-O may function as a signaling molecule in response to oxidative stress and nutrients.

Results

Purification and Sequence Determination of *E. coli* fRMsr. Extracts of the *E. coli* MsrA$^-$B$^-$ strain were used to identify the origins of the remaining Msr activity (7, 8). The extract was fractionated by ammonium sulfate precipitation and a series of chromatographic columns. At each step of this process, the enzymatic activity for the reduction of free MetO was measured by using the nitroprusside assay. In this assay, Met reacts with the nitroprusside molecule, leading to a change in absorbance at 540 nm (7, 8). Ammonium sulfate was found to inhibit the Msr activity, thus requiring dialysis of the samples before analysis. Only those fractions that exhibited the highest specific activity were pooled at each step of the purification.

The last stage of the fRMsr purification used a Resource Q anion-exchange column. A comparison of the protein distribution within the fractions by SDS/PAGE analysis with the Msr activity profile revealed that only one group of protein bands showed correspondence. The putative fRMsr bands were excised and digested in-gel with trypsin. The resulting peptide fragments were

Author contributions: Z.L., H.W. and W.T.L. designed research; Z.L., L.C.J., H.W., and M.O.L. performed research; Z.L., H.W., N.B., and W.T.L. analyzed data; and Z.L. and W.T.L. wrote the paper.

The authors declare no conflict of interest.

Abbreviations: fRMsr, free Met-(*R*)-O reductase; Met, methionine; MetO, methionine sulfoxide; MMTS, methyl methanethiosulfonate; Msr, methionine sulfoxide reductases; Trx, thioredoxin; TrxR, thioredoxin reductase.

[‡]To whom correspondence should be addressed. E-mail: hweissba@fau.edu.

This article contains supporting information online at www.pnas.org/cgi/content/full/0703774104/DC1.

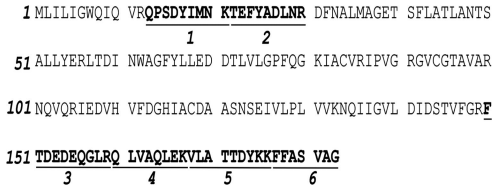

Fig. 1. Sequence of *E. coli* fRMsr. Six tryptic fragments were identified by mass spectrometry from *E. coli* fRMsr purified from MsrA^{-}B^{-} cells. The peptides are indicated in bold, underlined, and labeled 1–6. The identified sequence corresponds to the hypothetical *E. coli* protein NP_288269 and *E. coli* yebR of unknown function.

analyzed by reverse-phase HPLC coupled to the electrospray interface of a Bruker (Newark, DE) Esquire HCT ion-trap mass spectrometer. The acquired peptide mass finger prints were queried against a database of eubacteria proteins, using an in-house MASCOT server. Six peptide matches with significant molecular weight search scores were made to the hypothetical *E. coli* protein NP_288269 (Fig. 1): (*i*) QPSDYIMNK (*m*/*z*, 548.3; charge, +2); (*ii*) TEFYADLNR (*m*/*z*, 564.2; charge, +2); (*iii*) FTDEDEQGLR (*m*/*z*, 605.2; charge, + 2); (*iv*) QLVAQLEK (*m*/*z*, 465.3; charge, +2); (*v*) VLATTDYK (*m*/*z*, 456.2; charge, + 2); (*vi*) FFASVAG (*m*/*z*, 698.2; charge, +1). The NP_288269 protein has also been called the yebR protein (P76270) and classified as having an unknown function.

Purification of Recombinant fRMsr. The yebR gene was amplified by the PCR, using chromosomal DNA from *E. coli* strain JM109 as a template. This gene codes for an ≈20-kDa protein. The PCR product was cloned into a modified pET19 expression vector containing an N-terminal His-tag and intervening enterokinase and PreScission (Amersham Pharmacia, Little Chalfont, U.K.) protease cleavage sites (Fig. 2*A*). Upon expression in *E. coli* BL21(DE3) cells, the construct should result in the production of a protein ≈24 kDa long. Nickel NTA, gel filtration, and anion exchange columns were used to purify the protein to homogeneity. To our surprise, ≈18- and ≈24-kDa fRMsr species were observed by SDS/PAGE analysis. Mass spectrometry, N-terminal sequencing, and Western blot analysis, using an anti-His tag antibody (Fig. 2*B*), confirmed that the 18-kDa fMsr does not contain the His-tag and begins with residue Met-19. The 24-kDa fMsr was found to contain the His-tag. Both species exhibited the same Msr activity with the nitroprusside assay and eluted at a higher molecular weight than expected on the gel filtration column. The 18-kDa species was analyzed by analytical ultracentrifugation at 0.3 mg ml^{-1} and found to have an apparent molecular weight of 36 kDa (data not shown). The addition of DTT had no affect on the oligomeric state. At this time, it is not clear why the 18-kDa species was produced, although a weak ribosome binding site sequence is present upstream of Met-19. Moreover, it is not clear how the 18-kDa species was able to attach to the nickel NTA column, because it does not contain a His-tag. The 18-kDa fRMsr was used for the subsequent kinetic assays because of its high purity and abundance.

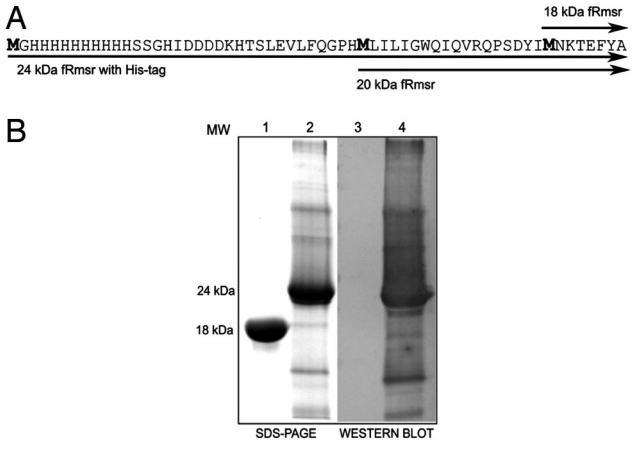

Fig. 2. Expression construct and purification of recombinant *E. coli* fRMsr. (*A*) N-terminal sequence for the expression construct. Expression from this modified pET19 vector yields a 24-kDa species containing an N-terminal, His_{10}-tag with intervening PreScission protease and enterokinase cleavage sites. The protein sequence from the second Met corresponds to the full-length *E. coli* fRMsr in Fig. 1. Initiation of protein synthesis at the third Met would result in a protein 18 kDa long. (*B*) SDS/PAGE and Western blot analysis of purified 18- and 24-kDa fRMsr species. Lanes 1 and 3, 18-kDa fRMsr; lane 2 and 4, 24-kDa fRMsr. An anti-His tag antibody (Qiagen, Valencia, CA) positively labels only the 24-kDa fRMsr.

Substrate Specificity and Kinetic Analysis of fRMsr. The reductase activity of *E. coli* MsrA and MsrB utilizes the reducing equivalents from the Trx-TrxR-NADPH redox system (12, 13). MsrA and MsrB show stereospecificity toward their substrates and can reduce both free MetO and peptide bound MetO, although the activity of MsrB against free Met-(*R*)-O is much lower (3, 4, 14, 15). The reducing system and substrate specificity of *E. coli* fRMsr were tested by measuring the reductase activity under a variety of assay conditions including substrates of different size and epimers of MetO. In these experiments, activity was measured by monitoring the decrease in NADPH absorbance at 340 nm. fRMsr exhibited the highest Met-(*R*)-O reductase activity when all components of the NADPH-TrxR-Trx system were present in the reaction (data not shown). Recombinant fRMsr also showed strict substrate specificity toward free Met-(*R*)-O (Fig. 3*A*). The enzyme was not able to reduce Met-(*S*)-O, Met sulfone, dimethyl sulfoxide, or MetO when present in the synthetic peptide NH_2-Pro-Thr-Ser-Met-(RS)-O-Glu-His-Val-NH_2. In contrast, the control proteins bovine MsrA (bMsrA) and *Neisseria gonorrhoeae* MsrB (ngMsrB) were able to reduce the free and peptide forms of Met-(*S*)-O and Met-(*R*)-O, respectively.

To compare the reductase activity of fRMsr to other Msr enzymes, a steady-state kinetic analysis of *E. coli* fRMsr activity was performed by using the NADPH-TrxR-Trx redox system. The rates of the reaction were determined from mixtures containing 0.5–6.5 mM Met-(*R*)-O, 2–30 μM eTrx, and 72 nM fRMsr. The resulting curves (Fig. 3*B*) were simultaneously fit to the Michaelis–Menten equation, using nonlinear regression analysis ($R^2 = 0.994$). The K_M value, turnover over number (k_{cat}), and catalytic efficiency (k_{cat}/K_M) for Met-(*R*)-O were determined to be 3.9 ± 0.4 mM, 6.9 ± 0.4 s^{-1}, and 1769 ± 181 M^{-1} s^{-1}, respectively. The K_M for *E. coli* Trx was 9.8 ± 0.9 μM.

Change in Free Thiol Content Associated with Met-(*R*)-O Reduction. The formation of intramolecular disulfide bonds are an integral component of the catalytic cycles of the MsrA enzymes and ngMsrB (3, 16). To investigate whether a similar scenario occurs in fRMsr, the free thiol content was determined by reaction with the small, thiol-labeling agent methyl methanethiosulfonate (MMTS) under different reaction conditions. fRMsr was pretreated with DTT (2 mM) for 10 min, followed by the direct addition of Met or Met-(*R*)-O (17 mM) (Table 1). The number of free sulfhydryl groups was then determined by the direct addition of excess MMTS (380 mM). Reaction of MMTS with a sulfhydryl group (-SH) results in the covalent attachment of the methylthiol group (-SCH_3, 47 Da) which can be readily monitored by MALDI-TOF mass spectrometry. The addition of DTT and Met (treatment 1) resulted in a molecular mass of 18,140 Da, a mass comparable with the theoretical mass of 18,121 Da for the 18-kDa fragment of fRMsr. The addition of MMTS (treatment 2) led to an increase in mass of 135 Da, indicating a complete labeling of all three Cys residues: Cys-84, Cys-94, and Cys-118 (numbering scheme based on the full-length 20-kDa sequence). The addition of Met-(*R*)-O (treatment 3) re-

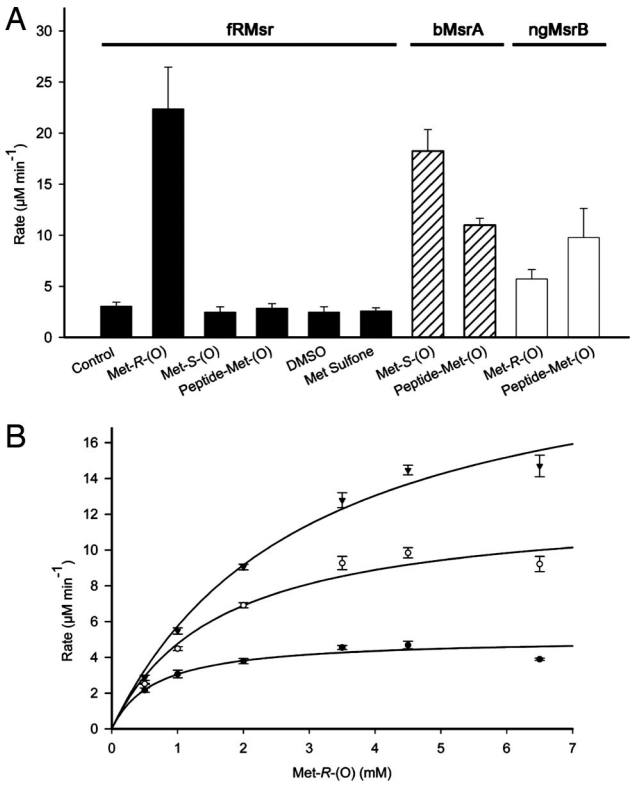

Fig. 3. Biochemical characterization of *E. coli* fRMsr. (*A*) Substrate specificity analysis of *E. coli* fRMsr. The rate observed for the control sample (no substrate) indicates the intrinsic NADPH oxidase rate of eTrxR. The reaction conditions were: fRMsr (0.102 μM), NADPH (250 μM), eTrxR (0.64 μM), eTrx (40 μM), bMsrA and ngMsrB (1.5 μM). The substrate concentration for the smaller substrates was 13 mM. For the peptide, a concentration of 26 mM was used, assuming that the proportion of Met-(*R*)-O and Met-(*S*)-O were equivalent. (*B*) Kinetic characterization of *E. coli* fRMsr. The reductase activity was assayed at various concentrations of purified Met-(*R*)-O. The reaction system included fRMsr (0.072 μM), NADPH (250 μM), and eTrxR (0.64 μM) and eTrx (2 μM, 7 μM, 30 μM; increasing in concentration from the bottom curve to the top).

sulted in a mass increase of 158 Da, a mass consistent with the addition of one DTT molecule (152 Da). Treatment of this sample with MMTS (treatment 4) resulted in the addition of one methylthiol group. These observations suggest that a DTT molecule makes a disulfide-bonding interaction with two Cys residues of fRMsr. The addition of a stronger reductant Tris-(2-carboxyethyl)-phosphine·hydrochloride was able to collapse the DTT adduct (treatment 5).

Conservation and Structure of *E. coli* fRMsr. A BLAST search with the *E. coli* fRMsr sequence against the current nonredundant sequence database revealed many homologous sequences (>350), including many hypothetical proteins or proteins of unknown function. Sequence identity ranges from 32% to 98%. Trp-62, Tyr-66, Cys-84, Cys-94, Cys-118, Glu-125, Asp-141, and Asp-143 of *E.coli* fRMsr are preserved across Eubacteria, Archaea, and the Fungi kingdom of the Eukaryota domain [see the representative alignment shown in supporting information (SI) Fig. 5]. As discussed below, these residues are part of the active site and belong to the motif: [W/F]-*X*-GFY-$X_{(6-14)}$-L-X_6-G-X_3-[C/D/E]-$X_{(7-8)}$-G-[V/I/L]-C-X_{14}-V-X_8-C-X_6-E-X_3-P-X_{11}-D-[V/I/L]-D-X_{10}-D, where X_n represents any amino acid and number of residues. It is important to note that humans and other higher eukaryotes do not have the fRMsr gene, and that most bacteria and yeast contain only one fRMsr gene.

During the sequence analysis, it was also discovered that the 2.1-Å crystal structure of *E. coli* fRMsr has been determined by the Structural GenomiX bacterial genomics project [Protein Data Bank (PDB) code 1VHM] (17). It is important to note, however, that the protein was still classified as having no known function. Thus, the present study assigns a function to the fRMsr scaffold. The structure of *E. coli* fRMsr is composed of six β-strands, three α-helices, and two prominent surface loops (Fig. 4*A*). Loop 1 is located between β2 and β3, and loop 2 is located between β4 and β5. The formation of a disulfide bond between Cys-84 of loop 1 and Cys-118 of loop 2 closes off the top of a cavity. Within this cavity a 2-(N-morpholino) ethanesulfonic acid (Mes) molecule was trapped from the crystallization milieu (Fig. 4*B*). The sulfonic acid moiety is closest to Cys-94, which is located at the N terminus of an α-helix. The remainder of the cavity is lined with Trp-62, Tyr-66, Ile-87, Val-93, Ile-116, Ala-117, Glu-125, Asp-141, and Asp-143 (Fig. 4*C*).

Discussion

Previous studies using the wild-type, MsrA$^-$, and MsrA$^-$B$^-$ strains of *E. coli* and *S. cerevisiae* have suggested that there are several remaining soluble and membrane-associated MetO reductases (7–10, 18, 19). In this study, we have identified an enzyme abbreviated fRMsr that is stereo- and size-specific for reducing free Met-(*R*)-O to Met (Fig. 3*A*). This strict substrate size selectivity contrasts with the broad specificity exhibited by the MsrA and MsrB reductases. For example, MsrA can reduce free L-MetO, D-MetO, N-Ac-L-MetO, dimethyl sulfoxide, L-ethionine sulfoxide, sulindac, and both enzymes can reduce MetO within a peptide or protein context (20–22). The kinetic parameters for recombinant *E. coli* fRMsr were determined for comparison with other MetO reductases. The fRMsr enzyme can readily use the *E. coli* Trx-TrxR-NADPH system as a source of electrons in the reaction (Fig. 3*B*) (K_M for eTrx was 9.8 μM) and exhibits a catalytic efficiency (k_{cat}/K_M) of 1,769 $M^{-1}s^{-1}$ for free L-Met-(*R*)-O. This value is comparable with the efficiencies observed for eMsrA (2,020 $M^{-1}s^{-1}$), ngMsrA (1,200 $M^{-1}s^{-1}$), and biotin sulfoxide reductase

Table 1. Mass spectrometric analysis of the reactivity of fRMsr thiols groups

Treatment*	Molecular mass, Da	Δ mass, Da	$-SCH_3$, no.†	DTT, no.†
(1) +DTT + Met − MMTS	18,140	0	0	0
(2) +DTT + Met + MMTS	18,275	135	3	0
(3) +DTT + Met-*R*(O) − MMTS	18,298	158	0	1
(4) +DTT + Met-*R*(O) + MMTS	18,342	202	1	1
(5) (3) + TCEP	18,140	0	0	0

*18 kDa fRMsr (20 μM) was incubated with a variety of compounds and analyzed by MALDI-TOF mass spectrometry as described in *Materials and Methods*. The DTT pretreatment results in the complete reduction of the enzyme. Addition of a methylthiol group ($-SCH_3$) from MMTS results in an increase in molecular mass of 46 Da (47 Da − 1 Da for the loss of H from the Cys thiol). The addition of a DTT molecule results in a theoretical increase in mass of 154 Da − 2 Da for each disulfide bond formed.

†The number of $-SCH_3$ groups and DTT molecules added to the fRMsr is based on comparison to treatment 1. Note that the addition of TCEP is able to reduce the Met-*R*(O)-induced DTT adduct.

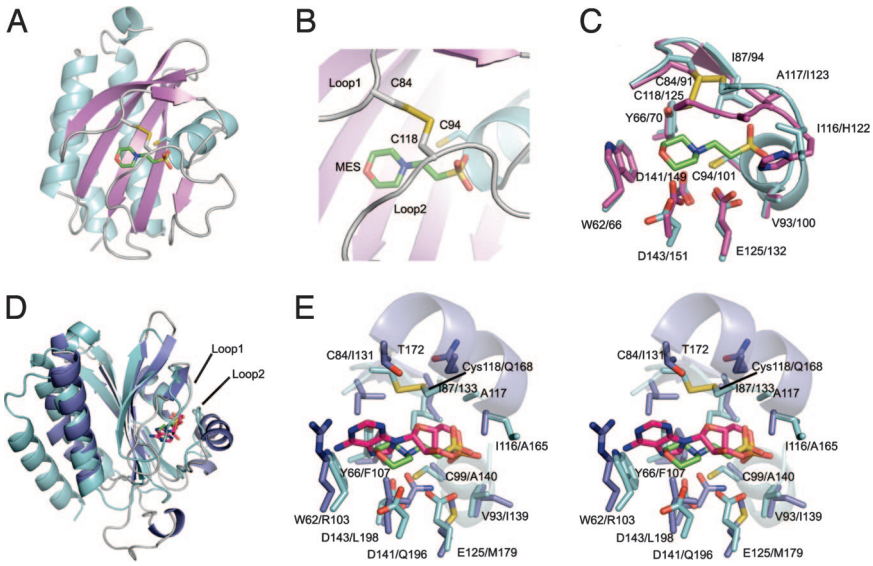

Fig. 4. *E. coli* fRMsr structure and comparisons with the GAF domains from yeast and *Anabaena*. (*A*) Overall fold of *E. coli* fRMsr. A Mes molecule (green carbon atoms; shown in stick rendering) is bound within an enclosed cavity (PDB code 1VHM) (17). (*B*) Close-up view of the Mes molecule and its proximity to three conserved Cys residues: Cys-84, Cys-94, and Cys-118. Surface loops 1 and 2 are linked together by a disulfide bond between Cys-84 and Cys-118. (*C*) Superposition of the Mes cavity residues for fRMsr (light blue carbon atoms) and the yeast YKG9 GAF domain (purple carbon atoms; PDB code 1F5M) (32). The first number in each label indicates the residue number for *E. coli* fRMsr. (*D*) Superposition of *E. coli* fRMsr and one of the GAF domains from *Anabena* adenylate cyclase (dark blue carbon atoms) complexed with cAMP (magenta carbon atoms; PDB code 1YKD) (41). Note the structural differences in loop 1 and in particular loop 2 of *Anabaena* which contains a α-helix. (*E*) Stereoview of the *E. coli* fRMsr and *Anabaena* cavities illustrating the lack of conservation of all residues, but the similar localization of the phosphate and sulfonate moieties.

(BisC, 3,137 $M^{-1}s^{-1}$), a free Met-(*S*)-O reductase requiring a molybdenum cofactor instead of Cys thiols, against free MetO under steady-state conditions (23–25). The reduction efficiency of fRMsr is, however, 100- to 1,200-fold greater than ngMsrB (19 $M^{-1}s^{-1}$) and eMsrB (1.5 $M^{-1}s^{-1}$) even though these enzymes are also stereospecific for Met-(*R*)-O (3, 5, 24, 26). Only upon substitution of the active site Cys of human MsrB1 (also known as SelX) with seleno-Cys does the catalytic efficiency (2,280 $M^{-1}s^{-1}$) increase to the level of fRMsr (27, 28). These observations suggest that fRMsr is the predominant free Met-(*R*)-O reductase within bacteria and yeast. This possibility may figure prominently in ensuring sufficient quantities of Met for protein synthesis during periods of oxidative stress.

The crystal structure of *E. coli* fRMsr in complex with a Mes buffer molecule (Fig. 4) has been determined (17). The proximity of the Mes sulfonic acid group to Cys-94 and the disulfide bond between Cys-84 and Cys-118 is reminiscent of the arrangement of active site residues in bMsrA and eMsrA (4, 14). In the structure of bMsrA, Cys-72 of the MsrA signature motif, Gly-71-Cys-Phe-Trp-Gly-75, is also located at the apex of a α-helix. In one crystal form, a DTT molecule was fortuitously trapped on both ends of the molecule by disulfide bonds to Cys-72 and Cys-218. Based on the DTT binding mode, a model for Met-(*S*)-O binding was generated. As a result, Tyr-103, Tyr-155, and Glu-115 were proposed to form a hydrophilic environment for the oxygen atom of the sulfoxide moiety. In addition, Trp-74 was thought to provide the key hydrophobic contact to the ε-methyl group of Met-(*S*)-O. Although it is clear that the overall folds of bMsrA and *E. coli* fRMsr are unrelated, it is possible that the residues which line the fRMsr active site function in a similar manner to residues in bMsrA. One particularly surprising finding was that Trp-62 is not adjacent to Cys-94 in three-dimensional space (Fig. 4*C*) as it is in bMsrA and the MsrB family members (4, 15). Nonetheless, the similar catalytic efficiency between these two classes of MetO reductases and the observation of unusual DTT adducts (Table 1) further supports their similarity. In both cases, the formation of the DTT adducts is most likely a consequence of the presence of a high concentration of DTT and the close proximity of two Cys thiols. The presence of Asp-141, Asp-143, and Glu-125 at the bottom of the cavity may provide the selectivity for the free, positively charged amino group of Met-(*R*)-O.

Based on these observations and the mechanistic similarities between the MsrA and MsrB reductases, the fRMsr catalytic reaction may proceed through the nucleophilic attack of Cys-94 onto the sulfur atom of Met-(*R*)-O. The collapse of the resulting intermediate would result in the formation of a Cys sulfenic acid (Cys-94-SOH). Our attempts to verify the formation of this intermediate by dimedone treatment were undoubtedly thwarted by the inability of the dimedone molecule (140 Da) to access the enclosed cavity during catalysis (29). The lack of conservation of Cys-84 in some organisms (SI Fig. 5) suggests that the Cys sulfenic intermediate immediately reacts with Cys-118 to form a disulfide bond. For those organisms with Cys-84, a thiol-disulfide exchange reaction could occur and lead to the Cys-84-Cys-118 disulfide bond observed in the crystal structure. This scenario would also be consistent with the reaction schemes for the MsrA enzymes that contain three Cys thiols (3). The disulfide bond would then be reduced by the Trx-TrxR-NADPH system. Additional structural and mutagenesis studies are necessary to evaluate the binding mode of substrate, the rearrangement of loops 1 and 2, and to test the role of active site residues during catalysis. It is clear, however, that part of the structural origins for the selectivity of fRMsr for free Met-(*R*)-O, and not peptide MetO as seen for MsrA and MsrB, is the enclosed nature of the active site.

A search of the DALI database with the *E. coli* fRMsr structure revealed several homologs that belong to the GAF domain family, a large group of sensor domains originally identified in mammalian cGMP-binding phosphodiesterases (e.g., PDE-2A), *Anabaena* adenylyl cyclases, and the *E. coli* transcription factor FhlA (30–33). GAF domains are typically found in tandem upstream of a variety of output domains. GAF domains play key roles in cyclic nucleotide signaling via adenylate cyclases and phosphodiesterases, transcription, phototransduction via the binding of bilin and flavin chromophores, and nitric oxide signaling (34–40). The first crystal

structure of a GAF domain was determined for the yeast protein YKG9 (PDB code 1F5M) (32), which shares 37% sequence identity with *E. coli* fRMsr. A superposition of the two crystal structures (Fig. 4*C*) (1.67 Å rmsd for C_α carbon atoms) reveals that all of the residues of the fRMsr active site motif are conserved, particularly the three Cys residues and the loop1/loop 2 disulfide bond. The only changes in the cavity involved the following substitutions: I-116/His-122 and Ala-117/I-123. Based on the strong correspondence to *E. coli* fRMsr, we propose that the yeast protein YKG9 is a free Met-(*R*)-O reductase. This proposal is consistent with the inability of YKG9 to bind cyclic nucleotides, a key function of many other GAF domains. Similarly, we have observed that the reductase activity of *E. coli* fRMsr is not inhibited by the addition of 12 mM AMP, GMP, cAMP, or cGMP (data not shown).

A comparison of *E. coli* fRMsr with one of the GAF domains of *Anabaena* adenylate cyclase (residues 79–230; PDB code 1YKD) reveals a clear structural basis for the observed ligand preferences (40, 41). The *Anabaena* GAF domain binds cAMP, exhibits 22% sequence identity to *E.coli* fRMsr and superimposes with an rmsd of 1.44 Å for C_α carbon atoms (Fig. 4*D*). The loop 1 and loop 2 motifs of both *E. coli* and the putative yeast fRMsr are replaced by a β-strand and a α-helix, respectively. Moreover, all of the residues of the cavity have been substituted between the enzymes (Fig. 4*E*). It is intriguing, however, that the location of the phosphate group of cAMP and the sulfonate group of the Mes molecule essentially superimpose. This observation suggests that the chemical and physical properties of this region of the cavity may be maintained for certain GAF ligand types, providing some additional support for this position being the binding site of the sulfoxide moiety of Met-(*R*)-O.

As mentioned above, one other key feature of GAF domains is that they are typically found in tandem (31). Moreover, the tandem GAF domains of *Anabaena* adenylate cyclase and the mouse phosphodiesterase 2A, for example, dimerize (i.e., four GAF domains total) via different interfaces (40, 41). As a result, these GAF dimers most likely interact with and modulate their downstream catalytic domains in unique ways. *E. coli* and yeast fRMsr also form a unique dimer as shown by their crystal structures and the analytical ultracentrifugation data for the *E. coli* enzyme. It is tempting to speculate that fRMsr in bacteria and yeast interacts with and modulates one or more proteins. These binding partners may include the downstream ProQ, a ProP transporter effector, in *E. coli* and an upstream putative homolog to the transcriptional regulator PaiB in *S. cerevisiae* as determined via The SEED server (www.theseed.org) (42, 43). Further support for this notion comes from the observation that in some organisms the fRMsr domain is fused to another domain. For example, in *Trypanosoma cruzi* and *Leishmania major*, the C terminus of fRMsr domain is fused to a TIP41-like domain, a domain important in nutrient signaling in yeast and the target of rampamycin (TOR) pathway (44, 45).

In summary, the identification of *E. coli* fRMsr has resulted in the determination of a molecule, Met-(*R*)-O, which can be added to the ligand recognition portfolio of GAF domains. The enzyme has strict specificity for Met-(*R*)-O, can use the Trx-TrxR-NAPDH system for reducing equivalents during catalysis and is as efficient as other Met(O) reductases. It appears that fRMsr may exploit a similar reaction scheme to the MsrA and MsrB Met(O) reductases. Therefore, by inference, the free Met pools, like Met within proteins (46), may protect bacterial and yeast cells by scavenging reactive oxygen species during host defense responses and other environmental challenges by the formation of Met(O). Although speculative, the binding and reduction of free Met(O) by the fRMsr GAF domain may function as a key element in cell signaling in response to oxidative stress and nutrients.

Materials and Methods

The method of Lavine was used to prepare and purify Met-(R)-O and Met-(S)-O (8, 47). The Met-(*R*)-O had ≈6% contamination with Met-(*S*)-O, but the Met-(*S*)-O was free of Met-(*R*)-O. *E. coli* Trx and TrxR were purified as N-terminal His-tag fusions, using the modified modified pET19 vector described below for recombinant fRMsr, and nickel NTA-affinity chromatography. For eTrx, the His-tag was removed by PreScission protease treatment and the protein further purified by size-exclusion chromatography, using 50 mM Hepes (pH 7.5) and 100 mM NaCl as the elution buffer. For eTrxR, the His-tag was not removed, and the protein was further purified by using a Blue Sepharose 6 FF column (GE Healthcare, Little Chalfont, U.K.) (48). Bovine MsrA and the MsrB domain from *N. gonorrhoeae* were purified as reported in refs. 16 and 49. The peptide substrate was synthesized by the Wake Forest University School of Medicine Protein Analysis Core Lab facility.

Purification of fRMsr from MsrA$^-$B$^-$ *E. coli* Cells. Approximately 76 g of MsrA$^-$B$^-$ *E. coli* cells (8) were obtained from five 10-liter fermentation cultures grown at 37°C in LB broth containing kanamycin and chloramphenicol at a concentration of 50 and 34 μg ml^{-1}, respectively. The cell pellets were homogenized in 200 ml of cell lysis buffer (10 mM Hepes, pH 7.5/10 mM $MgCl_2$/10 mM NH_4Cl) containing two EDTA-free protease inhibitor tablets (Roche Diagnostics, Indianapolis, IN). The supernatant was treated with 2.5% (wt/vol) streptomycin sulfate to remove DNA and further fractionated by a series of ammonium sulfate cuts: 30%, 40%, 50%, 60%, 70%, and 80%. Each pellet was resuspended in 10 ml of cell lysis buffer and dialyzed overnight against buffer A (50 mM Hepes, pH 7). The fractions with the highest specific activity as determined by the nitroprusside assay (7, 8, 18) and the Pierce (Rockford, IL) protein assay were applied to a DEAE column (130 ml) preequilibrated with buffer A. Proteins were eluted with 800 ml linear gradient from 0–100% of buffer B (50 mM Hepes, pH 7/1 M NaCl). The fRMsr-containing fractions were subsequently fractionated by Superdex75 (50 mM Hepes, pH 7/100 mM NaCl) and Resource Q (linear gradient from 10–40% buffer B/50 mM Hepes, pH 7/1 M NaCl) columns (GE Healthcare) at a flow rate of 1 ml min^{-1}.

Identification of fRMsr by Mass Spectrometry. SDS/PAGE gel plugs corresponding to the enzymatic activity of fRMsr were manually excised and rinsed consecutively with 200 μl of 50% acetonitrile until the Coomassie stain was completely removed. The gel pieces were dried under vacuum. Protein disulfide bonds were reduced and alkylated by the serial addition of 10 μl of 10 mM DTT and 10 μl of 50 mM iodoacetamide. The gel pieces were washed, minced in 200 μl of 100 mM NH_4HCO_3, and dehydrated by the addition of 100% acetonitrile. Gel pieces were rehydrated with 6 μl of activated trypsin (0.020 μg/μl) and incubated for 15 min at 37°C. The gel pieces were then covered with 50 μl of 50 mM NH_4HCO_3 and incubated overnight at 37°C.

Samples (5 μl) were loaded onto a precolumn (0.3 × 1.0 mm, 100 Å, PepMap C-18) for desalting and concentration at a flow rate of 35 μl min^{-1}, using mobile phase A (5% acetonitrile containing 0.1% formic acid). Peptides were eluted and separated on a nanoanalytical column (75 μm × 15 cm, 100 Å, PepMap C-18) at a flow rate of 200 nl min^{-1}, using a linear gradient from 5−40% mobile phase B (95% acetonitrile containing 0.08% formic acid) over 40 min. The peptides were ionized by nanoelectrospray and subjected to MS/MS analysis in a Bruker Esquire HCT ion trap mass spectrometer. MS survey data from *m/z* 375 to 1,300 were acquired. The MS/MS data were screened against bacterial sequences in the MSDB protein sequence database (Imperial College School of Medicine, London, U.K.), using MASCOT software (Matrix Science, London, U.K.). The search parameters were set such that that the enzyme specificity was set to trypsin with up to one missed cleavage. Carboxamidomethyl-cysteine and Met (oxidation) were also used as fixed and variable modifications, respectively. The mass tolerance was set to 1.0 Da for both parent and fragment ions. A probability-based molecular weight search algorithm [MOWSE score = $-10 \times \log(P)$] was used as a scoring

system, where P is the probability that an observed match is a random event. Therefore, the observed score of 295 indicates identity between the peptides observed and the *E. coli* fRMsr sequence.

Purification of Recombinant *E. coli* fRMsr. The fRMsr gene was amplified from the chromosomal DNA of *E. coli* strain JM109, using the PCR and primers containing flanking NdeI and BamHI restriction sites. The fMsr gene product was cloned into a modified pET19 vector containing an N-terminal His-tag and an intervening PreScission Protease cleavage site. BL21(DE3) *E. coli* cells containing the expression vector were grown in a 10-liter fermenter with 50 μg ml^{-1} ampicillin. When the OD_{600} of the culture reached 1.0, the temperature was decreased to 16°C, the agitation was decreased to 250 rpm, and IPTG was added to a concentration of 0.25 mM. The cells were harvested the following morning by centrifugation and stored at −80°C. *E. coli* fRMsr was then purified by using our standard protocol for nickel NTA-agarose column chromatography (16). The fractions corresponding to fRMsr were concentrated and loaded onto a 200-ml Superdex 75 gel filtration column. The resulting profile contained two species of fRMsr: the full-length 24-kDa protein and a truncated 18-kDa species. These species were separated by using the previous Resource Q column and gradient. The fRMsr species were estimated to be >99% pure by SDS/PAGE analysis, concentrated, aliquoted, and stored at −80°C. The theoretical extinction coefficient at 280 nm for each fRMsr species was calculated by using the Expasy Protparam Tool (Swiss Institute of Bioinformatics, Basel, Switzerland): 24 kDa fRMsr, 18,450 M^{-1} cm^{-1}; 18 kDa fRMsr, 11,460 M^{-1} cm^{-1}. Protein concentrations determined by using these parameters directly corresponded to the values determined by using the Pierce BCA assay.

Analysis of the fRMsr Reducing System and Substrate Specificity. The rate for the reduction of Met-(*R*)-O was determined by measuring the oxidation of NADPH at 340 nm within the eTrx-eTrxR-NADPH redox system. The NADPH extinction coefficient (6,220 $M^{-1}cm^{-1}$) was used to convert the observed rates to μM sec^{-1}. In this system, eTrx reduces fRMsr after the reduction of free Met-(*R*)-O. The triplicate reactions contained 20 mM Hepes (pH 7.4), 10 mM NaCl, 250 μM NADPH, 2−40 μM eTrx, 0.64 μM eTrxR, 0.5−26 mM substrate, and enzyme (72–102 nM fRMsr/1.5 μM bMsrA or ngMsrB) in a final volume of 170 μl. The reactions were carried out at 37°C and initiated by the addition of substrate. For the analysis of the peptide substrate, a concentration of 26 mM was used with the assumption that it contained equal proportions of the *S* and *R* forms of MetO. The resulting curves of the rate vs. [S] plot were simultaneously fit to a two-substrate model, using nonlinear regression analysis within the Enzyme Kinetics Module of SigmaPlot software, Version 9.0.

Determination of the Free Thiol Content by MALDI-TOF Mass Spectrometry. The number of free sulfhydryl groups of fRMsr was determined by reaction with MMTS (Pierce). Reaction of MMTS with a reduced sulfhydryl (Cys-SH) results in modification to dithiomethane (−S−SCH_3) with a theoretical mass increase of 46 Da for each methylthiol group added (-SCH_3). The increase of mass was measured with a delayed-extraction Bruker Autoflex MALDI-TOF mass spectrometer, using 10 mg ml^{-1} 3,5-dimethoxy-4-hydroxycinnamic acid, 30% acetonitrile, and 0.1% formic acid as the matrix solution. Pretreatment of fRMsr with 2 mM DTT at 37°C for 10 min was necessary to ensure the reduction of the disulfide bond that covers the active site. The reduced protein was then treated with Met, Met-(*R*)-O, Tris-(2-carboxyethyl)-phosphine·hydrochloride, or excess MMTS at 37°C for 1 h in a variety of combinations to assess the thiol-disulfide state of fRMsr during catalysis.

We thank Mark Morris (Protein Analysis Core Lab, Wake Forest University) for his help in the proteomics analyses and Dr. Daphna Sagher (Center for Molecular Biology and Biotechnology, Florida Atlantic University) for assay verification of the purified recombinant protein. This work was supported by developmental funds from Wake Forest University School of Medicine (to W.T.L.).

1. Vogt W (1995) *Free Radic Biol Med* 18:93–105.
2. Brot N, Weissbach H (2000) *Biopolymers* 55:288–296.
3. Boschi-Muller S, Olry A, Antoine M, Branlant G (2005) *Biochim Biophys Acta* 1703:231–238.
4. Kauffmann B, Aubry A, Favier F (2005) *Biochim Biophys Acta* 1703:249–260.
5. Grimaud R, Ezraty B, Mitchell JK, Lafitte D, Briand C, Derrick PJ, Barras F (2001) *J Biol Chem* 276:48915–48920.
6. Weissbach H, Etienne F, Hoshi T, Heinemann SH, Lowther WT, Matthews B, St John G, Nathan C, Brot N (2002) *Arch Biochem Biophys* 397:172–178.
7. Spector D, Etienne F, Brot N, Weissbach H (2003) *Biochem Biophys Res Commun* 302:284–289.
8. Etienne F, Spector D, Brot N, Weissbach H (2003) *Biochem Biophys Res Commun* 300:378–382.
9. Moskovitz J, Poston JM, Berlett BS, Nosworthy NJ, Szczepanowski R, Stadtman ER (2000) *J Biol Chem* 275:14167–14172.
10. Koc A, Gasch AP, Rutherford JC, Kim HY, Gladyshev VN (2004) *Proc Natl Acad Sci USA* 101:7999–8004.
11. Zoraghi R, Corbin JD, Francis SH (2004) *Mol Pharmacol* 65:267–278.
12. Brot N, Weissbach L, Werth J, Weissbach H (1981) *Proc Natl Acad Sci USA* 78:2155–2158.
13. Sagher D, Brunell D, Hejtmancik JF, Kantorow M, Brot N, Weissbach H (2006) *Proc Natl Acad Sci USA* 103:8656–8661.
14. Lowther WT, Brot N, Weissbach H, Matthews BW (2000) *Biochemistry* 39:13307–13312.
15. Lowther WT, Weissbach H, Etienne F, Brot N, Matthews BW (2002) *Nat Struct Biol* 9:348–352.
16. Lowther WT, Brot N, Weissbach H, Honek JF, Matthews BW (2000) *Proc Natl Acad Sci USA* 97:6463–6468.
17. Badger J, Sauder JM, Adams JM, Antonysamy S, Bain K, Bergseid MG, Buchanan SG, Buchanan MD, Batiyenko Y, Christopher JA, *et al.* (2005) *Proteins* 60:787–796.
18. Ejiri SI, Weissbach H, Brot N (1979) *J Bacteriol* 139:161–164.
19. Ejiri SI, Weissbach H, Brot N (1980) *Anal Biochem* 102:393–398.
20. Moskovitz J, Weissbach H, Brot N (1996) *Proc Natl Acad Sci USA* 93:2095–2099.
21. Etienne F, Resnick L, Sagher D, Brot N, Weissbach H (2003) *Biochem Biophys Res Commun* 312:1005–1010.
22. Weissbach H, Resnick L, Brot N (2005) *Biochim Biophys Acta* 1703:203–212.
23. Boschi-Muller S, Azza S, Branlant G (2001) *Protein Sci* 10:2272–2279.
24. Olry A, Boschi-Muller S, Marraud M, Sanglier-Cianferani S, Van Dorsselear A, Branlant G (2002) *J Biol Chem* 277:12016–12022.
25. Ezraty B, Bos J, Barras F, Aussel L (2005) *J Bacteriol* 187:231–237.
26. Ezraty B, Aussel L, Barras F (2005) *Biochim Biophys Acta* 1703:221–229.
27. Kim HY, Gladyshev VN (2004) *Mol Biol Cell* 15:1055–1064.
28. Bar-Noy S, Moskovitz J (2002) *Biochem Biophys Res Commun* 297:956–961.
29. Boschi-Muller S, Azza S, Sanglier-Cianferani S, Talfournier F, Van Dorsselear A, Branlant G (2000) *J Biol Chem* 275:35908–35913.
30. Aravind L, Ponting CP (1997) *Trends Biochem Sci* 22:458–459.
31. Hurley JH (2003) *Sci STKE* 2003(164):PE1.
32. Ho YS, Burden LM, Hurley JH (2000) *EMBO J* 19:5288–5299.
33. Holm L, Sander C (1993) *J Mol Biol* 233:123–138.
34. Kanacher T, Schultz A, Linder JU, Schultz JE (2002) *EMBO J* 21:3672–3680.
35. Martinez SE, Wu AY, Glavas NA, Tang XB, Turley S, Hol WG, Beavo JA (2002) *Proc Natl Acad Sci USA* 99:13260–13265.
36. Crosson S, Moffat K (2001) *Proc Natl Acad Sci USA* 98:2995–3000.
37. Wagner JR, Brunzelle JS, Forest KT, Vierstra RD (2005) *Nature* 438:325–331.
38. D'Autreaux B, Tucker NP, Dixon R, Spiro S (2005) *Nature* 437:769–772.
39. Sardiwal S, Kendall SL, Movahedzadeh F, Rison SC, Stoker NG, Djordjevic S (2005) *J Mol Biol* 353:929–936.
40. Bruder S, Linder JU, Martinez SE, Zheng N, Beavo JA, Schultz JE (2005) *Proc Natl Acad Sci USA* 102:3088–3092.
41. Martinez SE, Bruder S, Schultz A, Zheng N, Schultz JE, Beavo JA, Linder JU (2005) *Proc Natl Acad Sci USA* 102:3082–3087.
42. Kunte HJ, Crane RA, Culham DE, Richmond D, Wood JM (1999) *J Bacteriol* 181:1537–1543.
43. Overbeek R, Begley T, Butler RM, Choudhuri JV, Chuang HY, Cohoon M, de Crecy-Lagard V, Diaz N, Disz T, Edwards R, *et al.* (2005) *Nucleic Acids Res* 33:5691–5702.
44. Jacinto E, Guo B, Arndt KT, Schmelzle T, Hall MN (2001) *Mol Cell* 8:1017–1026.
45. Jacinto E, Hall MN (2003) *Nat Rev Mol Cell Biol* 4:117–126.
46. Levine RL, Mosoni L, Berlett BS, Stadtman ER (1996) *Proc Natl Acad Sci USA* 93:15036–15040.
47. Lavine TF (1947) *J Biol Chem* 169:477–491.
48. Poole LB, Godzik A, Nayeem A, Schmitt JD (2000) *Biochemistry* 39:6602–6615.
49. Brot N, Collet JF, Johnson LC, Jonsson TJ, Weissbach H, Lowther WT (2006) *J Biol Chem* 281:32668–32675.